Available online at www.sciencedirect.com
ScienceDirect
International Journal of Solids and Structures 43 (2006) 7145–7165
INTERNATIONAL JOURNAL OF SOLIDS and STRUCTURES
www.elsevier.com/locate/ijsolstr

Shape optimization for elasto-plastic deformation under shakedown conditions

K. Wiechmann *, E. Stein

Institute of Mechanics and Computational Mechanics, University of Hannover, Appelstr. 9 A, D-30167 Hannover, Germany

Received 4 June 2005; received in revised form 20 March 2006
Available online 28 March 2006

Abstract

An integrated approach for all necessary variations within direct analysis, variational design sensitivity analysis and shakedown analysis based on Melan's static shakedown theorem for linear unlimited kinematic hardening material behavior is formulated. Using an adequate formulation of the optimization problem of shakedown analysis the necessary variations of residuals, objectives and constraints can be derived easily. Subsequent discretizations w.r.t. displacements and geometry using e.g. isoparametric finite elements yield the well known 'tangent stiffness matrix' and 'tangent sensitivity matrix', as well as the corresponding matrices for the variation of the Lagrangian-functional which are discussed in detail. Remarks on the computer implementation and numerical examples show the efficiency of the proposed formulation. Important effects of shakedown conditions in shape optimization with elasto-plastic deformations are highlighted in a comparison with elastic and elasto-plastic material behavior and the necessity of applying shakedown conditions when optimizing structures with elasto-plastic deformations is concluded.

Keywords: Shape optimization; Elastic shakedown; Sensitivity analysis; Finite element analysis; Elasto-plastic deformation

1. Introduction

When optimizing structures with elasto-plastic deformations the fundamental problem occurs that deformations and stresses depend on the load path. Thus the optimized structure depends not only on the maximal loading but also on the loading history. The resulting shapes of structures optimized for the same maximal loading but different loading paths can be very diverse. This problem becomes even more aggravated if more than one load case must be considered. All possible load-combinations then form the so-called load domain. For elastic problems with multiple load cases it is permissible to consider only the corners of this load domain during optimization. The optimized structure will be safe for all possible load paths within this load domain. For elasto-plastic structures this is not the case. For optimization of these elasto-plastic structures with multiple load cases it is necessary to consider shakedown conditions.

* Corresponding author. Tel.: +49 5117625497; fax: +49 5117625496.
E-mail address: wiechmann@ibnm.uni-hannover.de (K. Wiechmann).

0020-7683/$ - see front matter
doi:10.1016/j.ijsolstr.2006.03.025

Shakedown of elasto-plastic systems subjected to variable loading occurs if after initial yielding plastification subsides and the system behaves elastically. This is due to the fact that a stationary residual stress field is formed and the total dissipated energy becomes stationary. Elastic shakedown (or simply shakedown) of a system is regarded as a safe state. In Section 3 the shakedown analysis of structures with unlimited linear kinematic hardening behavior is described.

It is important to know whether a system under given variable loading shakes down or not. But besides this other important tasks have to be considered. Such as the maximal possible enlargement of a load domain while the geometry of a given structure is kept fixed, the optimization (topology, shape design or material parameters) of the structure for a fixed load domain or the investigation of the sensitivity of the load factor with respect to changes in geometry, e.g. in order to take into account geometrical imperfections. All these problems require an efficient strategy for deriving sensitivity information, where special attention must be paid to the adequate numerical formulation and implementation to prevent the computations from becoming very time-consuming. In Section 4 the details for performing a variational design sensitivity analysis for shakedown problems with unlimited linear kinematic hardening are given. Classical Prandtl–Reuß elasto-plasticity for linear unlimited kinematic hardening with von Mises yield criterion is seen to be a relevant model problem with practical importance. For problems with this material behavior the shakedown analysis results in upper bounds for the shakedown load due to the fact that theoretically an infinite number of load cycles is permitted.

Shakedown analysis problems for two- and three-dimensional problems can normally only be solved numerically. In Section 5 the finite element discretization of the proposed formulation and details of the implementation concerning the algorithmic formulation of structural, sensitivity and shakedown analysis as well as storage requirements are discussed.

In Section 6 optimization problems for a square plate with a central circular hole in plane stress state are formulated, solved and compared for different material behavior and loading conditions.

2. State of the art

In 1932 Bleich (1932) was the first to formulate a shakedown theorem for simple hyperstatic systems consisting of elastic, perfectly plastic materials. This theorem was generalized by Melan (1938a,b) in 1938 to continua with elastic, perfectly plastic and linear unlimited kinematic hardening behavior. Koiter (1956) introduced a kinematic shakedown theorem for an elastic, perfectly plastic material in 1956, that was dual to Melan's static shakedown theorem. Since then extensions of these theorems for applications of thermoloadings, dynamic loadings, geometrically nonlinear effects, internal variables and nonlinear kinematic hardening have been carried out by different authors, see e.g. Corradi and Maier (1973), König (1969), Maier (1972), Prager (1956), Weichert (1986), Polizzotto et al. (1991) and Stein et al. (1993). Several papers were published concerning especially 2-D and 3-D problems, see Gokhfeld and Cherniavsky (1980), König (1966), Sawczuk (1969a), Sawczuk (1969b) and Leckie (1965). The shakedown investigation of these problems leads to grave mathematical problems. Thus, in most of these papers approximate solutions, based on the kinematic shakedown theorem of Koiter or on the assumption of a special failure form, were derived. But these solutions often lost their bounding character due to the fact that simplifying flow rules or wrong failure forms were estimated. Thus, the use of the finite element method was beneficial for the numerical treatment of shakedown problems, see Belytschko (1972), Corradi and Zavelani (1974), Nguyen Dang and Morelle (1981), Shen (1986) and Stein et al. (1993).

Structural optimization essentially needs an efficient strategy for performing the sensitivity analysis, i.e. for calculating the design variations of functionals modeling the objective and the constraints of the optimization problem. These demands are addressed within the so-called design sensitivity analysis which has been discussed in the literature for about the last three decades and especially for shape design sensitivity within the past 15 years. Two basic methods, i.e. the material derivative approach and the domain parametrization approach, have been used to derive the shape design sensitivity expressions. The material derivative approach dates back to 1981 (Céa, 1981; Zolésio, 1981) and was later extended to several different viewpoints. The domain parametrization method, also called control volume approach, was briefly introduced by Céa (1981), but did not gain popularity until Haber published a modified formulation in 1987. For a concise description and further hints to literature, see Tortorelli and Wang (1993) and Arora (1993). In Barthold and Stein (1996) a systematic reformulation of these two equivalent approaches was presented called the separation approach taking advantage of their merits but avoiding their drawbacks. The described approach was outlined for general hyperelastic material behavior with large strains. It was then extended to problems with linear and finite elasto-plastic material behavior for single load cases, see Wiechmann et al. (1997), Barthold and Wiechmann (1997) and Wiechmann and Barthold (1998).

Optimal plastic limit and shakedown design of bar structures with constraints on plastic deformation was investigated in Kaliszky and Lógó (1997). A first step towards an integrated formulation for general two- and three-dimensional elasto-plastic problems with multiple load cases under shakedown conditions was published first in Kaliszky and Lógó (2002) and Wiechmann et al. (2000).

3. Shakedown analysis of structures with unlimited linear kinematic hardening behavior

In Table 1 the constitutive equations of the classical Prandtl–Reuß elasto-plasticity with linear unlimited kinematic hardening and von Mises yield criterion are presented. Fig. 1 shows a typical stress–strain curve for this material in a cyclic test. The necessary shakedown condition for this material is that there exist at least one residual stress field $\bar{\boldsymbol{\rho}}(\boldsymbol{X})$ and one backstress field $\bar{\gamma}(\boldsymbol{X})$, such that

$$\Phi = \left\| \mathrm{dev}\left[\boldsymbol{\sigma}^{\mathrm{E}}(\boldsymbol{X},t) + \bar{\boldsymbol{\rho}}(\boldsymbol{X}) - \frac{2}{3}\bar{\gamma}(\boldsymbol{X})\right]\right\| - \sqrt{\frac{2}{3}}Y_0 \leqslant 0 \quad \forall \boldsymbol{X} \in \Omega_0 \tag{1}$$

is satisfied for all possible loads $\boldsymbol{P}(t)$ within the given load domain $\mathscr{M}$.

The following static shakedown theorem due to Melan states, that the necessary shakedown condition Eq. (1) in the sharper form Eq. (2) is also sufficient.

Table 1
Set of constitutive equations

Kinematics	$\boldsymbol{\varepsilon}^{\mathrm{e}} = \nabla^{\mathrm{s}}\boldsymbol{u} - \boldsymbol{\varepsilon}^{\mathrm{p}}$
	$e^{\mathrm{e}} = \boldsymbol{\varepsilon}^{\mathrm{e}} : \mathbf{1}, \quad \tilde{\boldsymbol{\varepsilon}}^{\mathrm{e}} = \mathrm{dev}[\boldsymbol{\varepsilon}^{\mathrm{e}}]$
1. Free energy	$\Psi = \widehat{\Psi}_{\mathrm{vol}}(e^{\mathrm{e}}) + \widehat{\Psi}_{\mathrm{iso}}(\tilde{\boldsymbol{\varepsilon}}^{\mathrm{e}}) + \widehat{K}(\boldsymbol{\alpha})$
	$= \frac{1}{2}\kappa(e^{\mathrm{e}})^2 + \mu\mathrm{tr}[\tilde{\boldsymbol{\varepsilon}}^{\mathrm{e}}\tilde{\boldsymbol{\varepsilon}}^{\mathrm{e}}] + \frac{1}{2}H\boldsymbol{\alpha} : \boldsymbol{\alpha}$
2. Macro stresses	$\boldsymbol{\sigma} = \partial_{e^{\mathrm{e}}}\widehat{\Psi}_{\mathrm{vol}} \cdot \mathbf{1} + \partial_{\tilde{\boldsymbol{\varepsilon}}^{\mathrm{e}}}\widehat{\Psi}_{\mathrm{iso}} : \mathbb{P} = \kappa e^{\mathrm{e}} \cdot \mathbf{1} + 2\mu\tilde{\boldsymbol{\varepsilon}}^{\mathrm{e}}$
3. Micro stresses	$\gamma = \partial_{\boldsymbol{\alpha}}\widehat{K}(\boldsymbol{\alpha}) = H\boldsymbol{\alpha}$
4. Plastic dissipation	$\mathscr{D}^{\mathrm{p}} = \boldsymbol{\sigma} : \dot{\boldsymbol{\varepsilon}}^{\mathrm{p}} - \gamma\dot{\boldsymbol{\alpha}} \geqslant 0$
5. Yield criterion	$\Phi = \widehat{\Phi}(\boldsymbol{\sigma}, \gamma) = \|\mathrm{dev}[\boldsymbol{\sigma}] - \frac{2}{3}\gamma\| - \sqrt{2/3}Y_0$
6. Flow rule	$\dot{\boldsymbol{\varepsilon}}^{\mathrm{p}} = \lambda[\mathrm{dev}[\boldsymbol{\sigma}] - \frac{2}{3}\gamma]/\|\mathrm{dev}[\boldsymbol{\sigma}] - \frac{2}{3}\gamma\| = \lambda\boldsymbol{n}$
7. Evolution	$\dot{\boldsymbol{\alpha}} = -\partial_{\gamma}\widehat{\Phi}(\boldsymbol{\sigma}, \gamma) = \frac{2}{3}\lambda\boldsymbol{n}$
8. Loading/unloading	$\lambda \geqslant 0, \ \Phi \leqslant 0, \ \lambda\Phi = 0$

μ: shear modulus, κ: bulk modulus, H: hardening parameter, Y_0: yield stress.

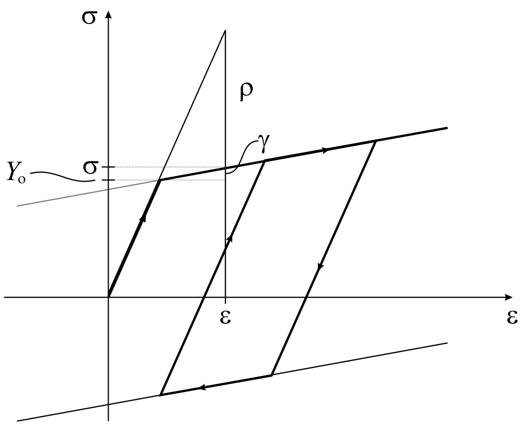

Fig. 1. Stress–strain curve for a material with linear unlimited kinematic hardening behavior.

Theorem 1. *If there exist a time-independent residual stress field* $\bar{\boldsymbol{\rho}}(\boldsymbol{X})$, *a time-independent backstress field* $\bar{\boldsymbol{\gamma}}(\boldsymbol{X})$ *and a factor* $m > 1$, *such that the condition*

$$\Phi[m\boldsymbol{\sigma}^{\mathrm{E}}(\boldsymbol{X},t), m\bar{\boldsymbol{\rho}}(\boldsymbol{X}), m\bar{\boldsymbol{\gamma}}(\boldsymbol{X})] \leqslant 0 \tag{2}$$

holds for all $\boldsymbol{P}(t)$ *in* $\mathscr{M}$ *and for all* $\boldsymbol{X}$ *in* Ω_0, *then the system will shake down.*

Based upon this static shakedown theorem an optimization problem can be formulated. We will investigate for a given system and a given load domain $\mathscr{M}$ how much the load domain $\mathscr{M}$ can be increased or must be decreased, respectively, such that the system will still shake down. The investigation of this optimization problem will be called shakedown analysis in the sequel. Introducing a load factor β we can reformulate the problem as follows: Calculate the maximal possible load factor β such that the system will shake down for the increased or decreased load domain $\mathscr{M}_\beta$, respectively. This optimization problem consists of the scalar valued objective β, the equilibrium conditions for the residual stresses $\bar{\boldsymbol{\rho}}$ and for the elastic stresses $\boldsymbol{\sigma}^{\mathrm{E}}$, i.e.

$$\mathscr{G}^{\rho} = \int_{\Omega_0} \mathrm{Grad}\,\boldsymbol{\eta} : \bar{\boldsymbol{\rho}}(\boldsymbol{X}) \mathrm{d}V_{\Omega_0}, \tag{3a}$$

$$\mathscr{G}^{\sigma^{\mathrm{E}}} = \int_{\Omega_0} \mathrm{Grad}\,\boldsymbol{\eta} : \boldsymbol{\sigma}^{\mathrm{E}}(\boldsymbol{X},t) \mathrm{d}V_{\Omega_0} - \int_{\Omega_0} \boldsymbol{\eta}\cdot\boldsymbol{b}(\boldsymbol{X},t)\mathrm{d}V_{\Omega_0} - \int_{\partial\Omega_0} \boldsymbol{\eta}\cdot\boldsymbol{p}(\boldsymbol{X},t)\mathrm{d}A_{\partial\Omega_0} \tag{3b}$$

(here, $\boldsymbol{\eta}$ denotes a test function and $\boldsymbol{b}$ and $\boldsymbol{p}$ are the applied loads) and the shakedown conditions Φ, i.e. Eq. (2). Thus the optimization problem can be represented as

$$\text{Objective} \quad \beta \rightarrow \max, \tag{4a}$$

$$\text{Constraints} \quad \mathscr{G}^{\rho} = 0, \tag{4b}$$

$$\mathscr{G}^{\sigma^{\mathrm{E}}} = 0, \tag{4c}$$

$$\Phi \leqslant 0 \ \forall\ \boldsymbol{X} \in \Omega_0, \quad \forall\ t > 0. \tag{4d}$$

Here, β is the objective function and the design variable of the optimization problem as well. Note the simple form of objective function as it consists only of this design variable β which must be maximized. The constraints $\mathscr{G}^{\sigma^{\mathrm{E}}}$, $\mathscr{G}^{\rho}$ and Φ depend on the elastic stresses $\boldsymbol{\sigma}^{\mathrm{E}}$, the residual stresses $\bar{\boldsymbol{\rho}}$ and the backstresses $\bar{\boldsymbol{\gamma}}$ as shown in Eqs. (2), (3a) and (3b). Due to the fact that the equilibrium conditions for the elastic stresses $\mathscr{G}^{\sigma^{\mathrm{E}}}$ and the shakedown conditions Φ must be fulfilled for any time $t > 0$ the number of constraints of this optimization problem is infinite.

In the frame of the classical shakedown theory the elastic stresses caused by the pseudo-time dependent sequence of loadings within the given load domain can be treated with time-independent stresses at the corners of a convex load domain. Thus, we assume that the load domain has the form of a convex n-dimensional polyhedron with M load vertices, see Fig. 2. Any point within the load domain can be described by a convex combination of the load vertices

$$\boldsymbol{P}(t) = \sum_{j=1}^{M} \alpha_j(t)\boldsymbol{P}(j), \quad \text{where} \quad \sum_{j=1}^{M} \alpha_j(t) = 1. \tag{5}$$

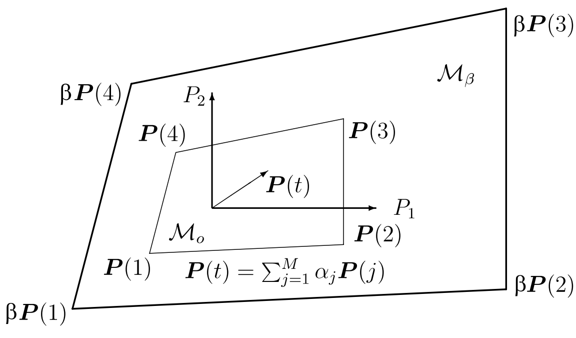

Fig. 2. Initial load domain $\mathscr{M}_0$ and maximized load domain $\mathscr{M}_\beta$ with $M = 4$ load vertices.

The time-dependent elastic stresses $\boldsymbol{\sigma}^{\mathrm{E}}$ can then be represented as

$$\boldsymbol{\sigma}^{\mathrm{E}}(t)=\sum_{j=1}^{M}\alpha_j(t)\boldsymbol{\sigma}^{\mathrm{E}}(j). \tag{6}$$

As a result of this formulation the number of shakedown conditions is limited to the number of load vertices of the load domain.

Taking advantage of this formulation Stein and Zhang (1992) introduced the following special optimization problem for unlimited linear kinematic hardening material behavior

$$\text{Objective} \quad \beta \rightarrow \max \tag{7a}$$

$$\text{Constraints} \quad \mathscr{G}_j(\boldsymbol{X},\boldsymbol{u}_j^0)=0, \tag{7b}$$

$$\Phi_j(\boldsymbol{X},\boldsymbol{u}_j^0,\beta,\bar{\boldsymbol{y}})\leqslant 0, \quad j\in[1,\ldots,M] \quad \forall \quad \boldsymbol{X}\in\Omega_0, \tag{7c}$$

where $\bar{\boldsymbol{\rho}}$ denotes the residual stresses, $\bar{\boldsymbol{\gamma}}$ denotes the backstresses and $\boldsymbol{y}$ is the difference of residual stresses and backstresses, i.e. $\boldsymbol{y}:=\bar{\boldsymbol{\rho}}-\bar{\boldsymbol{\gamma}}$, and will be denoted as internal stresses in the sequel. Note that the residual stresses $\boldsymbol{\rho}$ have to fulfill the homogeneous equilibrium conditions $\mathscr{G}^{\rho}=0$. The backstresses $\boldsymbol{\gamma}$ are unconstrained because we consider the simplified limit case of unlimited kinematic hardening behavior, cf. Stein et al. (1992) and Stein and Zhang (1992). For the shakedown analysis it is sufficient to show that one time-independent (constrained) residual stress field $\bar{\boldsymbol{\rho}}$ and one time-independent (unconstrained) backstress field $\bar{\boldsymbol{\gamma}}$ exist, cf. Theorem 1 but we are not interested in their explicit computation. Thus, by definition of the new variables $\boldsymbol{y}$, the shakedown conditions (2) can be reformulated in the form (7c). It is then sufficient to show the existence of one time-independent unconstrained internal stress field $\bar{\boldsymbol{y}}$, and thus the equality constraints for the backstresses $\mathscr{G}^{\rho}$ can be eliminated from the formulation. Furthermore no time-dependency occurs, whereas the optimization problem now depends on the displacements corresponding to the loading of the jth load vertex $\boldsymbol{u}_j^0$. $\mathscr{G}_j$ now denotes the weak form of equilibrium corresponding to the jth load vertex where the superscript σ^{E} is dropped for convenience. In order to simplify the notation this optimization problem is replaced by a Lagrangian-functional

$$L(\boldsymbol{X},\boldsymbol{u}_j^0,\boldsymbol{z},\boldsymbol{\mu},\boldsymbol{\lambda})=-\beta+\mu_j\mathscr{G}_j(\boldsymbol{X},\boldsymbol{u}_j^0)+\lambda_j\Phi_j(\boldsymbol{X},\boldsymbol{u}_j^0,\boldsymbol{z})\rightarrow \text{stat}, \tag{8}$$

where μ_j and λ_j are Lagrangian-multipliers for the equality and inequality constraints, respectively, and the vector $\boldsymbol{z}$ is the solution of the optimization problem and consists of the load factor β and the internal stresses $\boldsymbol{y}$, i.e. $\boldsymbol{z}^{\mathrm{T}}=[\beta,\boldsymbol{y}^{\mathrm{T}}]$. The Kuhn–Tucker conditions which are necessary for an optimal solution are

$$\mathscr{L}(\boldsymbol{X},\boldsymbol{u}_j^0,\boldsymbol{z},\boldsymbol{\mu},\boldsymbol{\lambda})=0, \tag{9a}$$

$$\mathscr{G}_j(\boldsymbol{X},\boldsymbol{u}_j^0)=0, \tag{9b}$$

$$\Phi_j(\boldsymbol{X},\boldsymbol{u}_j^0,\boldsymbol{z})\leqslant 0, \tag{9c}$$

$$\lambda_j\geqslant 0, \tag{9d}$$

$$\lambda_j\Phi_j=0. \tag{9e}$$

Here $\mathscr{L}$ is derived from the Lagrangian L by variation w.r.t. the primal unknowns $\boldsymbol{z}$, i.e. $\delta_z L=\epsilon\mathscr{L}$. A detailed presentation of Eq. (9a) for the chosen model problem is given in Eqs. (24a) and (24b). Note that in a shape optimization process the geometry field $\boldsymbol{X}$ is no longer fixed but depends on the choice of geometrical design variables. Thus, when shakedown constraints are considered in a shape optimization process the dependency of the Lagrangian-functional L on the field $\boldsymbol{X}$ must be considered. This general formulation of the optimization problem is the basis for a sensitivity analysis described in the next section.

4. Variational design sensitivity analysis

The sensitivity analysis of the objective function or the constraint functions under consideration can be performed with different methods. Our approach is based upon the variational design sensitivity analysis of the investigated functionals. This means the variations of the continuous formulation are calculated and then in a subsequent step they are discretized in order to get computable expressions. The main advantage of this methodology is that the sensitivity analysis can be formulated analogous to and consistent with the structural analysis and the shakedown analysis. The weak form of equilibrium and the Lagrangian-functional presented above are formulated for the continuous structure and are then being discretized. Thus, many formulations that were derived for and are being used for the direct analysis (structural analysis and shakedown analysis) can also be applied to the sensitivity analysis.

The separation approach to continuum mechanics based on convected coordinates, see Barthold and Stein (1996), yields a decomposition of the deformation mapping $\boldsymbol{x} = \boldsymbol{\varphi}(\boldsymbol{X}, t)$ into an independent geometry mapping $\boldsymbol{X} = \tilde{\boldsymbol{\psi}}(\boldsymbol{\Theta})$ and a displacement mapping $\boldsymbol{u} = \tilde{\boldsymbol{v}}(\boldsymbol{\Theta}, t)$, see Fig. 3. Different gradient operators can be defined, i.e. grad, Grad and GRAD, see Fig. 4, corresponding to the independent variables $\boldsymbol{x}$, $\boldsymbol{X}$ and $\boldsymbol{\Theta}$ of the considered domains Ω_t, Ω_0 and $\mathscr{T}_\Theta$, respectively. Furthermore, the convected basis vectors are $\widetilde{\boldsymbol{E}}_i$ on $\mathscr{T}_\Theta$, $\boldsymbol{G}_i := \partial \boldsymbol{X}/\partial \Theta^i$ on Ω_0 and $\boldsymbol{g}_i := \partial \boldsymbol{x}/\partial \Theta^i$ on Ω_t. Thus, the material displacement gradient can be decomposed as follows:

$$\boldsymbol{H} = \mathrm{Grad}\, \boldsymbol{v}(\boldsymbol{X}) = \mathrm{GRAD}\, \tilde{\boldsymbol{v}}(\boldsymbol{\Theta})[\mathrm{GRAD}\, \tilde{\boldsymbol{\psi}}(\boldsymbol{\Theta})]^{-1}. \tag{10}$$

The gradients $\mathrm{GRAD}\, \tilde{\boldsymbol{v}}(\boldsymbol{\Theta})$ and $\mathrm{GRAD}\, \tilde{\boldsymbol{\psi}}(\boldsymbol{\Theta})$ are used to decompose continuum mechanical tangent mappings and to perform pull back and push forward transformations between Ω_0 or Ω_t and the parameter space $\mathscr{T}_\Theta$. See Eq. (22) for details on deriving explicit expressions for the necessary variations for the chosen model problem.

4.1. Sensitivity analysis of shakedown analysis problems

4.1.1. General formulation

Sensitivity analysis of problems with shakedown conditions should be based on the chosen numerical implementation of the direct problem in order to obtain correct and consistent expressions and numerically efficient implementations. The key points of our approach are:

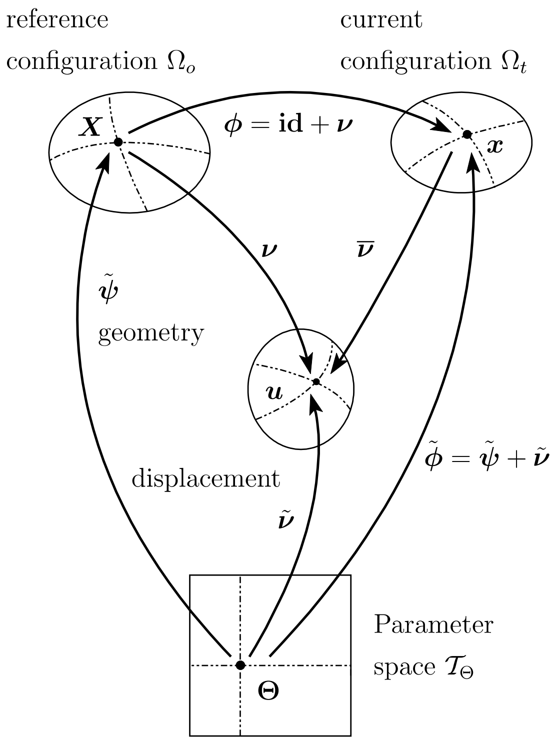

Fig. 3. Configurations and mappings in continuum mechanics.

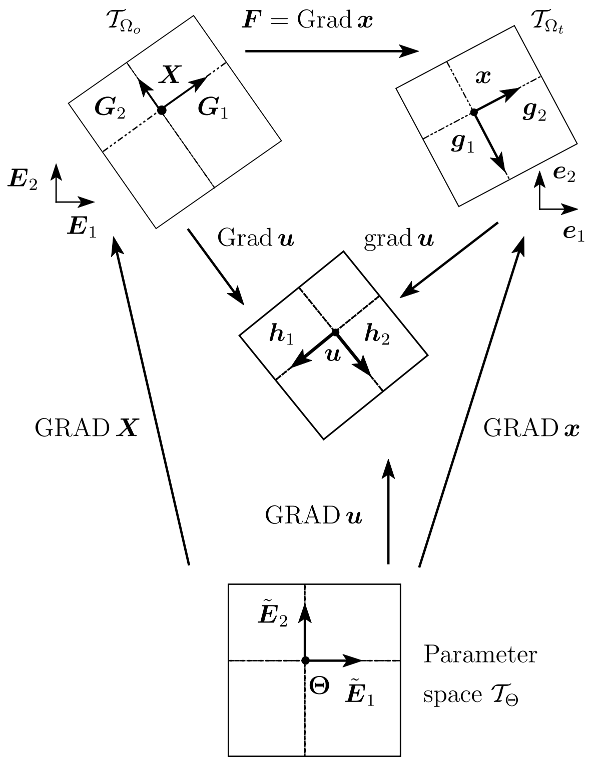

Fig. 4. Tangent mappings and transformation operators.

- The variation of the geometry mapping $\delta\boldsymbol{X}$ is assumed to be given.
- The equilibrium condition $\mathcal{G}_j = 0$ of the jth load vertex is derived by variation of the energy Π w.r.t. the displacement function, i.e. $\delta_u \Pi = \epsilon\mathcal{G}$. Here $\boldsymbol{\eta}$ are admissible test functions using the embedding $\tilde{\boldsymbol{u}} = \boldsymbol{u} + \epsilon\boldsymbol{\eta}$. The equilibrium condition is solved to compute the displacement mapping $\boldsymbol{u}_j^0$, i.e.

$$\mathcal{G}_j(\boldsymbol{\eta}, \boldsymbol{X}, \boldsymbol{u}_j^0) = 0. \tag{11}$$

- The optimality condition $\mathcal{L} = 0$ is derived by variation of the Lagrangian L w.r.t. the unknown function $\boldsymbol{z}$, i.e. $\delta_z L = \epsilon\mathcal{L}$. Here $\boldsymbol{\zeta}$ are admissible test functions using the embedding $\tilde{\boldsymbol{z}} = \boldsymbol{z} + \epsilon\boldsymbol{\zeta}$. The optimality condition is solved to calculate the solution of the shakedown analysis problem $\boldsymbol{z}$, where $\boldsymbol{z}^{\mathrm{T}} = [\beta, \boldsymbol{y}^{\mathrm{T}}]$, i.e.

$$\mathcal{L}(\boldsymbol{\zeta}, \boldsymbol{X}, \boldsymbol{u}_j^0, \boldsymbol{z}, \boldsymbol{\mu}, \boldsymbol{\lambda}) = 0. \tag{12}$$

- The variation of the equilibrium condition $\mathcal{G}_j = 0$ yields

$$0 = \delta_s\mathcal{G}_j + \delta_{u_j^0}\mathcal{G}_j = s_j(\boldsymbol{\eta}, \delta\boldsymbol{X}) + k_j(\boldsymbol{\eta}, \delta\boldsymbol{u}_j^0), \tag{13}$$

  where $s_j(\boldsymbol{\eta}, \delta\boldsymbol{X})$ denotes the 'tangent sensitivity' of the jth load vertex

$$s_j(\boldsymbol{\eta}, \delta\boldsymbol{X}) = \frac{\partial\mathcal{G}_j}{\partial\boldsymbol{X}}\delta\boldsymbol{X} \tag{14}$$

  and $k_j(\boldsymbol{\eta}, \delta\boldsymbol{u}_j^0)$ denotes the 'tangent stiffness' corresponding to the jth load vertex

$$k_j(\boldsymbol{\eta}, \delta\boldsymbol{u}_j^0) = \frac{\partial\mathcal{G}_j}{\partial\boldsymbol{u}_j^0}\delta\boldsymbol{u}_j^0. \tag{15}$$

- Thus, the variation of the displacement mapping $\delta\boldsymbol{u}_j^0$ is implicitly defined by Eq. (13) and can be represented as

$$\frac{\partial\mathcal{G}_j}{\partial\boldsymbol{u}_j^0}\delta\boldsymbol{u}_j^0 = -\frac{\partial\mathcal{G}_j}{\partial\boldsymbol{X}}\delta\boldsymbol{X}. \tag{16}$$

- The variation of the optimality condition $\mathscr{L} = 0$, see Eq. (12), yields

$$0 = \delta_z \mathscr{L} + \delta_s \mathscr{L} + \delta_{u_j^0} \mathscr{L} = l_z(\boldsymbol{\zeta}, \delta \boldsymbol{z}) + l_s(\boldsymbol{\zeta}, \delta \boldsymbol{X}) + l_{u_j^0}(\boldsymbol{\zeta}, \delta \boldsymbol{u}_j^0), \tag{17}$$

where three bilinear forms are being introduced. Here $l_z(\boldsymbol{\zeta}, \delta \boldsymbol{z})$ is known from shakedown analysis. It denotes the variation of $\mathscr{L}$ w.r.t. $\boldsymbol{z}$, i.e.

$$l_z(\boldsymbol{\zeta}, \delta \boldsymbol{z}) = \frac{\partial \mathscr{L}}{\partial \boldsymbol{z}} \delta \boldsymbol{z}. \tag{18}$$

The term $l_s(\boldsymbol{\zeta}, \delta \boldsymbol{X})$ denotes the variation of $\mathscr{L}$ w.r.t. geometry and can be represented as

$$l_s(\boldsymbol{\zeta}, \delta \boldsymbol{X}) = \frac{\partial \mathscr{L}}{\partial \boldsymbol{X}} \delta \boldsymbol{X}. \tag{19}$$

And finally $l_{u_j^0}(\boldsymbol{\zeta}, \delta \boldsymbol{u}_j^0)$ denotes the variation of $\mathscr{L}$ w.r.t. the displacements of the jth load vertex, i.e.

$$l_{u_j}(\boldsymbol{\zeta}, \delta \boldsymbol{u}_j^0) = \frac{\partial \mathscr{L}}{\partial \boldsymbol{u}_j^0} \delta \boldsymbol{u}_j^0. \tag{20}$$

- Thus, the variations of load factor $\delta\beta$ and internal stresses $\delta \boldsymbol{y}$ of the shakedown analysis problem are implicitly defined by Eq. (17) and can be represented by

$$\frac{\partial \mathscr{L}}{\partial \boldsymbol{z}} \delta \boldsymbol{z} = -\frac{\partial \mathscr{L}}{\partial \boldsymbol{X}} \delta \boldsymbol{X} - \frac{\partial \mathscr{L}}{\partial \boldsymbol{u}_j^0} \delta \boldsymbol{u}_j^0. \tag{21}$$

Using Eq. (16) the variation of the displacement field $\delta \boldsymbol{u}_j^0$ can be denoted in terms of the variation of the geometry mapping $\delta \boldsymbol{X}$ and thus, the variation of the solution of the shakedown analysis problem $\delta \boldsymbol{z}^{\mathrm{T}} = [\delta\beta, \delta \boldsymbol{y}^{\mathrm{T}}]$, i.e. the variation of the load factor and the internal stresses, can finally be denoted in terms of $\delta \boldsymbol{X}$, too.

4.1.2. Formulation for the chosen model problem

To derive the variational formulation presented above the total variation of the weak form of equilibrium and of the optimality condition must be supplied, see Eqs. (11) and (17).

4.1.2.1. Variation of the weak form of equilibrium. For notational convenience we limit our attention to the internal part of the weak form of equilibrium

$$\mathscr{G}_j^{\mathrm{int}} = \int_{\Omega_0} \operatorname{Grad} \boldsymbol{\eta} : \boldsymbol{\sigma}_j^{\mathrm{E}} \mathrm{d}V_{\Omega_0}. \tag{22}$$

Its total variation consists of partial variations w.r.t. displacements and w.r.t. geometry and it is computed by a 'pull-back–variation–push forward' – scheme, i.e.

$$\begin{aligned} \delta \mathscr{G}_j^{\mathrm{int}} &= \delta \left[\int_{\mathscr{T}_\Theta} \operatorname{Grad} \boldsymbol{\eta} : \boldsymbol{\sigma}_j^{\mathrm{E}} J_\Psi \,\mathrm{d}V_{\mathscr{T}_\Theta} \right] = \int_{\mathscr{T}_\Theta} \operatorname{Grad} \boldsymbol{\eta} : \delta[\boldsymbol{\sigma}_j^{\mathrm{E}}] J_\Psi + \boldsymbol{\sigma}_j^{\mathrm{E}} : \delta[\operatorname{Grad} \boldsymbol{\eta}] J_\Psi + \boldsymbol{\sigma}_j^{\mathrm{E}} : \operatorname{Grad} \boldsymbol{\eta} \delta[J_\Psi] \mathrm{d}V_{\mathscr{T}_\Theta} \\ &= \int_{\Omega_0} \operatorname{Grad} \boldsymbol{\eta} : \mathbb{C}^{\mathrm{E}} : [\operatorname{Grad} \delta \boldsymbol{u}_j^0 - \operatorname{Grad} \boldsymbol{\eta} \operatorname{Grad} \delta \boldsymbol{X}] \mathrm{d}V_{\Omega_0} - \int_{\Omega_0} \boldsymbol{\sigma}_j^{\mathrm{E}} : \operatorname{Grad} \boldsymbol{\eta} \operatorname{Grad} \delta \boldsymbol{X} \,\mathrm{d}V_{\Omega_0} \\ &\quad + \int_{\Omega_0} \boldsymbol{\sigma}_j^{\mathrm{E}} : \operatorname{Grad} \boldsymbol{\eta} \operatorname{Div} \delta \boldsymbol{X} \,\mathrm{d}V_{\Omega_0}. \end{aligned} \tag{23}$$

The first part of this total variation corresponds to the partial variation of the elastic stresses $\boldsymbol{\sigma}^{\mathrm{E}}$ w.r.t. the displacements $\boldsymbol{u}_j^0$ of the jth load vertex. This part is well known from finite element analysis. The last three terms correspond to the variation of the elastic stresses $\boldsymbol{\sigma}^{\mathrm{E}}$, the material gradient of the test-functions $\operatorname{Grad} \boldsymbol{\eta}$ and the Jacobi-determinant of the transformation onto the parameter space J_Ψ w.r.t. geometry $\boldsymbol{X}$.

4.1.2.2. Variation of the optimality condition. This variation consists of the partial variations w.r.t. $\boldsymbol{z}$, $\boldsymbol{X}$ and $\boldsymbol{u}_j^0$ and is equal to zero. The optimality condition $\mathscr{L}$ of the Lagrangian-functional L consists of parts variations w.r.t. the load factor denoted as $\mathscr{L}_\beta$ and w.r.t. the internal stresses denoted as $\mathscr{L}_y$, i.e. $\mathscr{L} = \mathscr{L}_\beta + \mathscr{L}_y$. For the chosen model problem these terms read

$$\mathscr{L}_\beta = -\alpha + \lambda_j[2\boldsymbol{\sigma}_j : \mathbb{P} : \boldsymbol{\sigma}_j^{\mathrm{E}}\alpha], \tag{24a}$$

$$\mathscr{L}_y = +\lambda_j[2\boldsymbol{\sigma}_j : \mathbb{P} : \boldsymbol{\gamma}]. \tag{24b}$$

Here α and $\boldsymbol{\gamma}$ are admissible test functions using the embedding $\tilde{\beta} = \beta + \epsilon\alpha$ and $\tilde{\boldsymbol{y}} = \boldsymbol{y} + \epsilon\boldsymbol{\gamma}$, respectively.

Thus, the total variation of the optimality condition $\delta\mathscr{L}$ can be split additively into two parts: the total variation of $\mathscr{L}_\beta$, which results from the partial variation of the Lagrangian-functional L w.r.t. the load factor β, and the total variation of $\mathscr{L}_y$, which results from the partial variation of the Lagrangian-functional L w.r.t. the internal stresses $\boldsymbol{y}$. Each of these total variations $\delta\mathscr{L}_\beta$ and $\delta\mathscr{L}_y$ consists of partial variations w.r.t. the load factor β, the internal stresses $\boldsymbol{y}$, the displacements of the jth load vertex $\boldsymbol{u}_j^0$ and the geometry $\boldsymbol{X}$ as indicated in the following equations:

$$\begin{aligned}
\delta\mathscr{L}_\beta = {} & 2\lambda_j\alpha\boldsymbol{\sigma}_j^{\mathrm{E}} : \mathbb{P} : \mathbb{I} : \boldsymbol{\sigma}_j^{\mathrm{E}}\delta\beta && \Big|\ \delta\beta \\
& + 2\lambda_j\alpha\boldsymbol{\sigma}_j^{\mathrm{E}} : \mathbb{P} : \mathbb{I} : \delta\boldsymbol{y} && \Big|\ \delta\boldsymbol{y} \\
& + 2\lambda_j\alpha\boldsymbol{\sigma}_j : \mathbb{P} : \mathbb{C}^{\mathrm{E}} : \mathrm{Grad}\,\delta\boldsymbol{u}_j^0 && \\
& + 2\lambda_j\alpha\boldsymbol{\sigma}_j^{\mathrm{E}} : \mathbb{P} : \beta\mathbb{C}^{\mathrm{E}} : \mathrm{Grad}\,\delta\boldsymbol{u}_j^0 && \Big|\ \delta\boldsymbol{u}_j^0 \\
& - 2\lambda_j\alpha\boldsymbol{\sigma}_j : \mathbb{P} : \mathbb{C}^{\mathrm{E}} : \boldsymbol{H}_j\mathrm{Grad}\,\delta\boldsymbol{X} && \\
& - 2\lambda_j\alpha\boldsymbol{\sigma}_j^{\mathrm{E}} : \mathbb{P} : \beta\mathbb{C}^{\mathrm{E}} : \boldsymbol{H}_j\mathrm{Grad}\,\delta\boldsymbol{X}, && \Big|\ \delta\boldsymbol{X}
\end{aligned} \tag{25a}$$

$$\begin{aligned}
\delta\mathscr{L}_y = {} & 2\lambda_j\boldsymbol{\gamma} : \mathbb{P} : \mathbb{I} : \boldsymbol{\sigma}_j^{\mathrm{E}}\delta\beta && \Big|\ \delta\beta \\
& + 2\lambda_j\boldsymbol{\gamma} : \mathbb{P} : \mathbb{I} : \delta\boldsymbol{y} && \Big|\ \delta\boldsymbol{y} \\
& + 2\lambda_j\boldsymbol{\gamma} : \mathbb{P} : \beta\mathbb{C}^{\mathrm{E}} : \mathrm{Grad}\,\delta\boldsymbol{u}_j^0 && \Big|\ \delta\boldsymbol{u}_j^0 \\
& - 2\lambda_j\boldsymbol{\gamma} : \mathbb{P} : \beta\mathbb{C}^{\mathrm{E}} : \boldsymbol{H}_j\mathrm{Grad}\,\delta\boldsymbol{X}, && \Big|\ \delta\boldsymbol{X}
\end{aligned} \tag{25b}$$

where the following notation is used:

$\mathbb{C}^{\mathrm{E}}$: linear elastic tangent operator,
$\mathbb{I}$: fourth-order unity tensor,
$\mathbb{P}$: fourth-order deviatoric projection tensor,
$\boldsymbol{H}_j$: displacement gradient for the jth load vertex.

Note that the structure of the derived variations is almost identical. Furthermore the partial variations of the functionals $\mathscr{L}_\beta$ and $\mathscr{L}_y$ w.r.t. the load factor β and w.r.t. the internal stresses $\boldsymbol{y}$ are required for solving the shakedown analysis problem and are already known. Thus, the only additional effort to perform sensitivity analysis is the computation of the partial variations w.r.t. displacements $\boldsymbol{u}_j^0$ corresponding to the jth load vertex and w.r.t. geometry $\boldsymbol{X}$.

5. Numerical solution of shakedown analysis problems with unlimited linear kinematic hardening using the finite element method

5.1. General considerations

The numerically efficient implementation of shakedown analysis problems is an important task due to the fact that normally a discretized optimization problem with very many constraints has to be analyzed. This is because in case of perfect plasticity or limited kinematic hardening the shakedown constraints must be calculated for every load vertex in every Gaussian point of the discretized structure. Thus, numerical solution procedures have been formulated like a reduced bases technique or a special SQP-algorithm, see Stein et al. (1992, 1990). Nevertheless it was shown by Stein and Zhang (1992) that for unlimited linear kinematic hardening the formulation of the optimization problem can be simplified because of the local nature of the failure of problems with this kind of material behavior.

The following strategy allows to take advantage of the special structure of the shakedown optimization problem

- In a first step the solution of the equilibrium conditions $\mathcal{G}_j = 0$ for any load vertex j is computed.
- Then the vectors of elastic stresses $\underline{\sigma}_j^{\mathrm{E}}(i)$ in any Gaussian point i of the discretized structure are being calculated.
- In a final step the solution of the global discretized shakedown optimization problem is calculated by solving local optimization problems in any Gaussian point based upon the following lemma, see Stein and Zhang (1992).

Lemma 2. *The global maximal load factor* β *of a shakedown analysis problem with unlimited linear kinematic hardening material behavior is given by*

$$\beta = \bar{\beta} \quad \text{with } \bar{\beta} = \min_{i=1,\mathrm{NGP}} \beta_i, \tag{26}$$

where β_i *is the solution of the local sub-problem defined in the ith Gaussian point*

$$\text{Objective} \qquad \beta_i \to \max, \tag{27a}$$

$$\text{Constraint} \quad \Phi[\beta_i \underline{\sigma}_j^{\mathrm{E}}(i) + \underline{y}(i)] \leqslant 0 \quad \forall \quad j = [1, \ldots, M]. \tag{27b}$$

Note that the structure of the local optimization problems is very simple because the number of constraints is equal to the number of load vertices. We adopt the solution strategy described above and formulate the sensitivity analysis consistent with this formulation, see Fig. 5. First of all the sensitivities of the elastic stresses are being computed and after the shakedown analysis problem has been solved its sensitivities are being calculated as well.

5.2. Finite element discretization

The continuous formulation derived in Section 4.1 is now being discretized by using a standard displacement formulation. Two expressions, the total variation of the weak form of equilibrium and the total variation of the optimality condition of the shakedown analysis problem, must be investigated.

The total variation of the weak form with respect to design using the introduced bilinear forms $s_j(\boldsymbol{\eta}, \delta\boldsymbol{X})$ and $k_j(\boldsymbol{\eta}, \delta\boldsymbol{u}_j^0)$ reads, see Eq. (13),

$$\delta\mathcal{G}_j = \delta_s\mathcal{G}_j + \delta_{u_j^0}\mathcal{G}_j = s_j(\boldsymbol{\eta}, \delta\boldsymbol{X}) + k_j(\boldsymbol{\eta}, \delta\boldsymbol{u}_j^0) = 0. \tag{28}$$

The FE-discretization with $\boldsymbol{\eta}^h$, $\delta\boldsymbol{u}^h$ and $\delta\boldsymbol{X}^h$ on each element domain leads to an approximation of the variation of the considered functionals by the derivative with respect to scalar valued design variables

$$\delta\mathcal{G}_j = 0 \to \frac{\mathrm{d}\mathcal{G}_j^h}{\mathrm{d}s} = \bigcup_{e=1}^{E}\{s_j^{e,h}(\boldsymbol{\eta}^h, \delta\boldsymbol{X}^h) + k_j^{e,h}(\boldsymbol{\eta}^h, \delta\boldsymbol{u}_j^{0,h})\} = \underline{\hat{\eta}}^{\mathrm{T}}\underline{S}_j\delta\underline{\widehat{X}} + \underline{\hat{\eta}}^{\mathrm{T}}\underline{K}_j\delta\underline{\hat{u}}_j^0 = \underline{\hat{\eta}}^{\mathrm{T}}\{\underline{S}_j\delta\underline{\widehat{X}} + \underline{K}_j\delta\underline{\hat{u}}_j^0\} = 0, \tag{29}$$

where underlined symbols denote matrices and vectors of the respective continuous quantities.

Thus, we obtain for each virtual node coordinate vector $\delta\underline{\widehat{X}} \in \mathbb{R}^k$ the induced virtual node displacement vector $\delta\underline{\hat{u}}_j^0 \in \mathbb{R}^n$

$$\delta\underline{\hat{u}}_j^0 = -\underline{K}_j^{-1}\underline{S}_j\delta\underline{\widehat{X}}, \tag{30}$$

where $\underline{K}_j$ is the global tangential stiffness matrix of order $(n \times n)$, $\underline{S}_j$ is the global tangential sensitivity matrix of order $(n \times k)$, n is the overall number of degrees of freedom and k is the overall number of coordinates, see Barthold and Stein (1997).

The total variation of optimality condition for any local sub-problem with respect to design using the introduced bilinear forms $l_z(\boldsymbol{\zeta}_i, \delta\boldsymbol{z}_i)$, $l_s(\boldsymbol{\zeta}_i, \delta\boldsymbol{X})$ and $l_{u_j^0}(\boldsymbol{\zeta}_i, \delta\boldsymbol{u}_j^0)$ reads, see Eq. (17),

$$\delta\mathcal{L}_i = \delta_z\mathcal{L}_i + \delta_s\mathcal{L}_i + \delta_{u_j^0}\mathcal{L}_i = l_z(\boldsymbol{\zeta}_i, \delta\boldsymbol{z}_i) + l_s(\boldsymbol{\zeta}_i, \delta\boldsymbol{X}) + l_{u_j^0}(\boldsymbol{\zeta}_i, \delta\boldsymbol{u}_j^0) = 0. \tag{31}$$

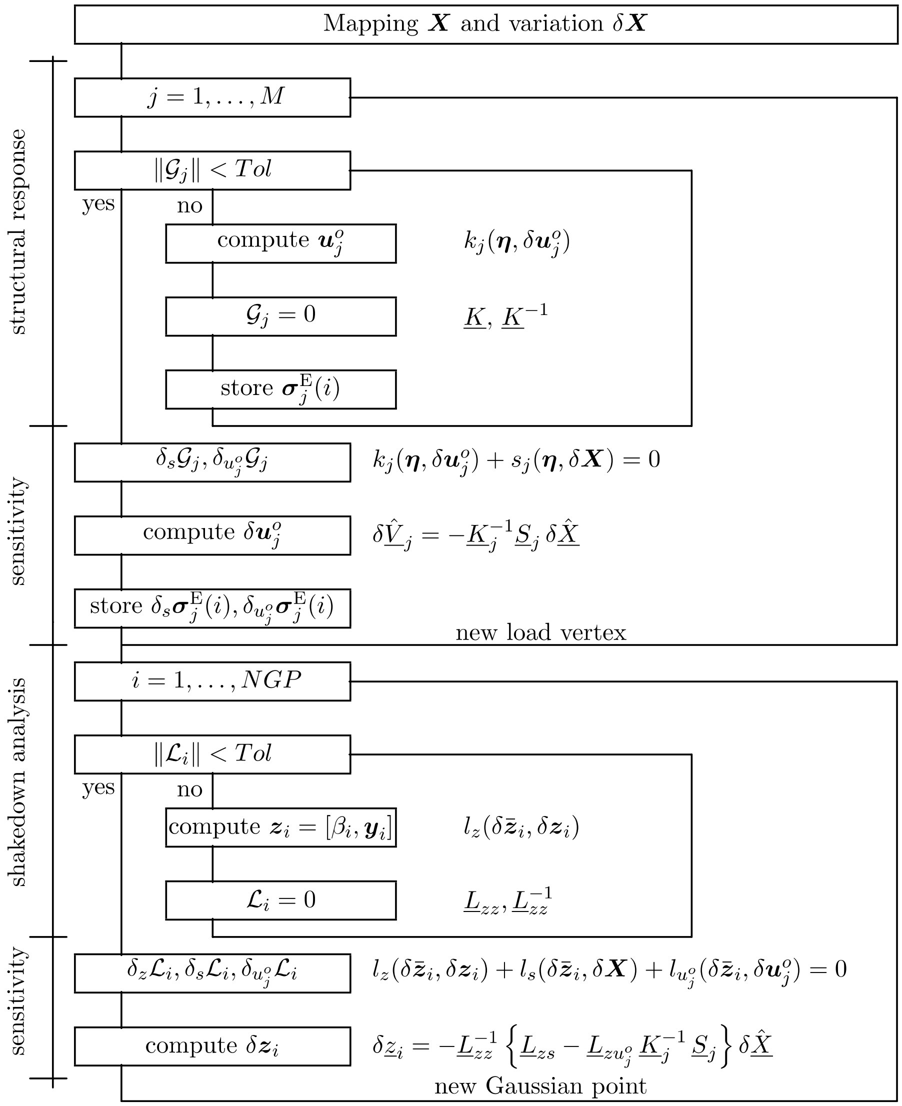

Fig. 5. Flow chart of structural analysis, sensitivity analysis and shakedown analysis.

The FE-discretization on each element domain leads to an approximation of the variation of the considered functionals by the derivative with respect to scalar valued design variables

$$\delta\mathscr{L}_i = 0 \rightarrow \frac{\mathrm{d}\mathscr{L}_i^h}{\mathrm{d}s} = \{l_z^{e,h}(\zeta_i^h, \delta z_i^h) + l_s^{e,h}(\zeta_i^h, \delta X^h) + l_{u_j^0}^{e,h}(\zeta_i^h, \delta u_j^{o,h})\} = \underline{\zeta}_i^{\mathrm{T}}\underline{L}_{zz}\delta\underline{\hat{z}}_i + \underline{\zeta}_i^{\mathrm{T}}\underline{L}_{zs}\delta\underline{\widehat{X}} + \underline{\zeta}_i^{\mathrm{T}}\underline{L}_{zu_j^0}\delta\underline{\hat{u}}_j^0$$
$$= \underline{\zeta}_i^{\mathrm{T}}\{\underline{L}_{zz}\delta\underline{\hat{z}}_i + \underline{L}_{zs}\delta\underline{\widehat{X}} + \underline{L}_{zu_j^0}\delta\underline{\hat{u}}_j^0\} = 0. \tag{32}$$

Thus, by using Eq. (30) we obtain for each virtual node coordinate vector $\delta\underline{\widehat{X}} \in \mathbb{R}^k$ the induced virtual vector $\delta\underline{\hat{z}} \in \mathbb{R}^l$

$$\delta\underline{\hat{z}} = -\underline{L}_{zz}^{-1}\left\{\underline{L}_{zs} - \underline{L}_{zu_j^0}\underline{K}_j^{-1}\underline{S}_j\right\}\delta\underline{\widehat{X}}, \tag{33}$$

where $\underline{L}_{zz}$ is the local Hessian matrix of order $(l \times l)$, $\underline{L}_{zs}$ is the local shakedown sensitivity matrix of order $(l \times k)$, $\underline{L}_{zu_j^0}$ is the local shakedown displacement matrix of order $(l \times n)$ and l is the number of unknowns of the local shakedown problem.

5.3. Storage requirements

Two different methods are suitable for the implementation of the shakedown analysis and its variation.

One way is to compute the global displacement vectors $\underline{u}_j^0$ and the elastic stress vectors $\underline{\sigma}_j^{\mathrm{E}}(i)$ at each Gaussian point i for each load vertex. The stress vectors $\underline{\sigma}_j^{\mathrm{E}}(i)$ as well as their total variations $\delta\underline{\sigma}_j^{\mathrm{E}}(i)$ must be stored to solve the shakedown analysis problem and the sensitivity analysis problem, respectively.

In order to minimize the storage required to perform shakedown analysis and its sensitivity analysis we use the following strategy instead. The vectors of the global displacements $\underline{u}_j^0$ are being stored for each load vertex $j = 1, \ldots, M$. The vectors of the elastic stresses $\underline{\sigma}_j^{\mathrm{E}}(i)$ at each Gaussian point are being recomputed in order to solve the local optimization problem. Additionally, in order to perform the sensitivity analysis, the total variation of the global displacement vectors $\delta\underline{u}_j^0$ is being stored for each load vertex $j = 1, \ldots, M$ and for each scalar valued design variable $s = 1, \ldots, \mathrm{NDV}$. The vectors of the total variation of the elastic stresses $\delta\underline{\sigma}_j^{\mathrm{E}}(i)$ at each Gaussian point are then being recomputed in order to solve the sensitivity analysis problem. Thus, implementing the sensitivity analysis for a shakedown analysis problem requires additional storage that is equal to that needed to implement the shakedown analysis multiplied with the number of design variables of the shape optimization problem.

6. Numerical examples

The formulation of sensitivity analysis of kinematically linear elasto-plastic materials as described above was implemented into a finite element research tool for inelastic analysis and optimization (INA-OPT). Computations of shakedown with unlimited linear kinematic hardening were performed which decouples the problem completely such that upper bounds (infinite number of load cycles) for low cycle fatigue were computed.

6.1. Square plate with a central circular hole – comparison of elastic and elasto-plastic optimization without and with shakedown constraints

The system depicted in Fig. 6 is a square plate with a central circular hole in plane stress state. The dimension of the whole structure is $a \times a = 20 \times 20$ cm. The diameter of the central hole is 2 cm. This structure is loaded by a uniformly distributed load p in the y-direction. Due to symmetry conditions only one quarter of the structure was investigated. It was discretized with standard two-dimensional isoparametric $Q1$-displacement elements, Fig. 8. The geometry of the circular hole was modeled by a Bézier curve with five control points, Fig. 7.

The material parameters used in the numerical analysis are shown in Table 2. With the initial geometry and material data three different optimization problems were investigated, Table 3. For all of these optimization problems the objective was to minimize the weight of the structure. The coordinates of 10 Bézier-points controlling the outer vertical and inner (hole) boundary of the plate were used as design variables, Fig. 7.

- *Example 1 (elastic optimization problem).* In the first of these optimization problems only elastic material behavior was considered and a static load $p = 3.0$ kN/cm was applied. Von Mises equivalent stress in the whole domain as well as maximum displacement u_y of the lower and upper edges $y = \pm\frac{a}{2}$ were restricted; the displacement condition is necessary for elasto-plastic deformation only and was not active for this optimization problem.
- *Example 2 (elasto-plastic optimization problem).* The same loading conditions and constraints were used for the second optimization problem but in this case elasto-plastic material behavior was considered. For details on the formulation of shape optimization of problems with linear elasto-plastic material behavior see e.g. Wiechmann et al. (1997).
- *Example 3 (shakedown optimization problem).* In the third optimization problem shakedown constraints were applied and a load domain was investigated with load vertices $-1.5 \leqslant p \leqslant 3.0$ kN/cm.

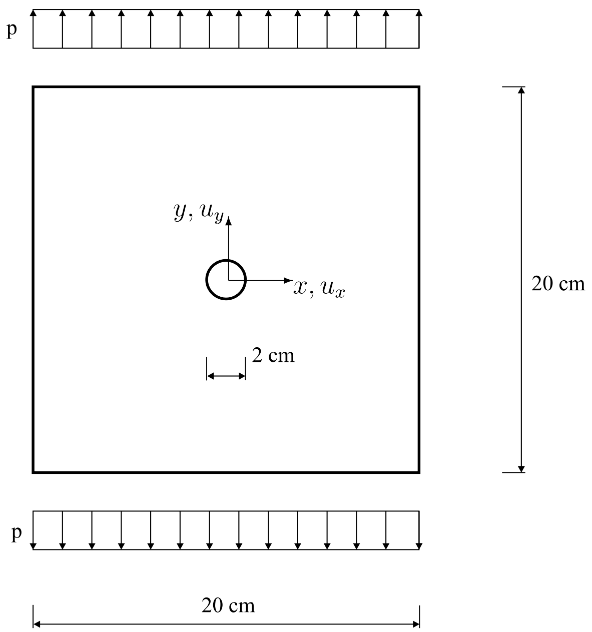

Fig. 6. Initial geometry and loading conditions.

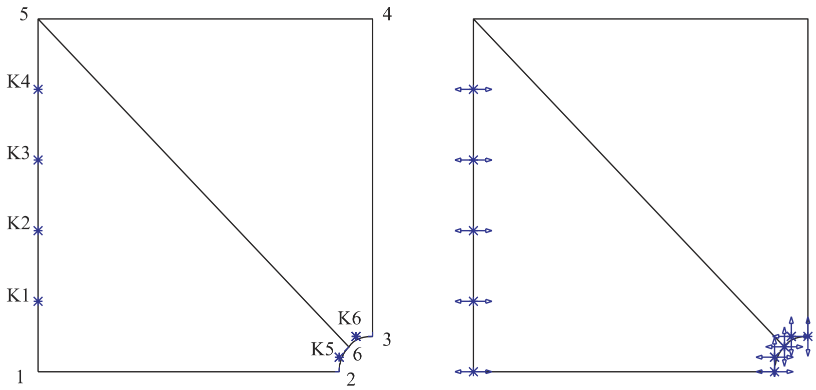

Fig. 7. Position of Bézier control-points and design variables.

Table 2
Material parameters

Young's modulus	$E = 206.90\ \text{kN/mm}^2$
Poisson's ratio	$\nu = 0.29$
Initial yield stress	$Y_0 = 0.45\ \text{kN/mm}^2$
Linear hardening	$H = 16.93\ \text{kN/mm}^2$

Table 3
Formulation of three different optimization problems

Example	Material behavior	Loading	Active constraints
1	Elastic	$p = 3.0$ kN/cm	$\boldsymbol{\sigma}$
2	Elasto-plastic	$p = 3.0$ kN/cm	$\boldsymbol{u}$
3	Elasto-plastic	$-1.5 \leqslant p \leqslant 3.0$ kN/cm	β

As depicted in Table 3 for example 1 (elastic material behavior) the stress constraints were active, whereas for example 2 (elasto-plastic material behavior) the displacement constraints were active. In example 3 (shakedown conditions) neither stresses nor displacements were restricted, but the maximal global load factor β was constrained.

All optimization problems (examples 1–3) were solved for three different discretizations (mesh a–c in Fig. 8). In Table 4 the weight of the optimized structures w.r.t. the weight of the initial design is shown. Summarizing, the results of the three optimization problems are as follows. The maximal reduction of weight is gained for example 2. The least saving of weight is obtained for example 1, Table 4. These results are discussed in detail in the following paragraphs.

In Fig. 9a–c the optimized structures for examples 1–3 (mesh c) are depicted. It can be seen that the optimal shapes of the structures become similar. During the optimization process the hole is extended in loading direction in order to reduce weight, whereas the diameter of the hole remains small perpendicular to the loading direction. Due to plastic yielding savings are larger in elasto-plastic optimization (Fig. 9b) than in elastic optimization (Fig. 9a). In example 3 (Fig. 9c) savings are larger than for the elastic behavior but less than for the elasto-plastic optimization.

In Fig. 10 results of elastic and elasto-plastic optimization are compared. Due to the reduction of stresses by plastic deformation the elasto-plastic optimization yields a higher utilization of the material and thus a considerable weight-reduction in comparison to the elastic problem. Note that the boundary of the hole becomes smoothly rounded in the elastic case for avoiding stress singularities, whereas non-smooth corners appear in the elasto-plastic case because elastic stress singularities are reduced.

In Fig. 11 results of elasto-plastic and shakedown optimization are compared. The difference of geometries for optimization with shakedown conditions with a load domain versus optimization for the elasto-plastic case with only one load case are relatively small. Thus the consideration of shakedown conditions yields only slightly higher weight than the consideration of only one elasto-plastic load case. The smaller savings for the shakedown problem with a load domain are due to the fact that the material cannot be utilized as much as in the plastic case where the resulting geometry is ideally suited for only one load case. But the resulting smoothness of the boundary of the hole in case of shakedown is a very important effect of shakedown analysis for application to low cycle fatigue where the resulting geometry is safe not only for one load case but for any load path with (theoretically) unlimited load cycles in the load domain.

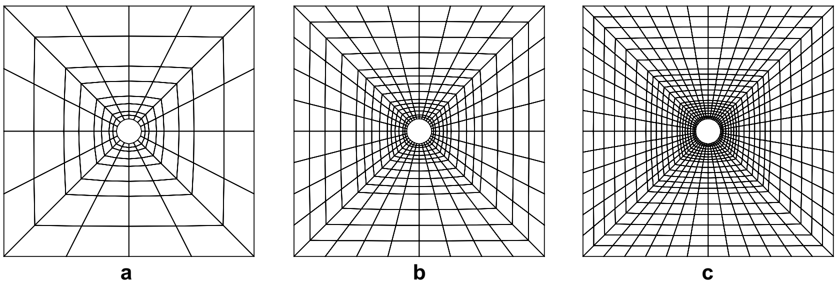

Fig. 8. Discretization of the initial design (only one quarter was considered for calculation due to symmetry); (a) mesh with (4×)32 elements; (b) mesh with (4×)112 elements; (c) mesh with (4×)240 elements.

Table 4
Weight of optimized structures in percentage of initial design

	Mesh a	Mesh b	Mesh c
Initial design (%)	100	100	100
Example 1 (%)	71	73	84
Example 2 (%)	67	67	67
Example 3 (%)	68	73	73

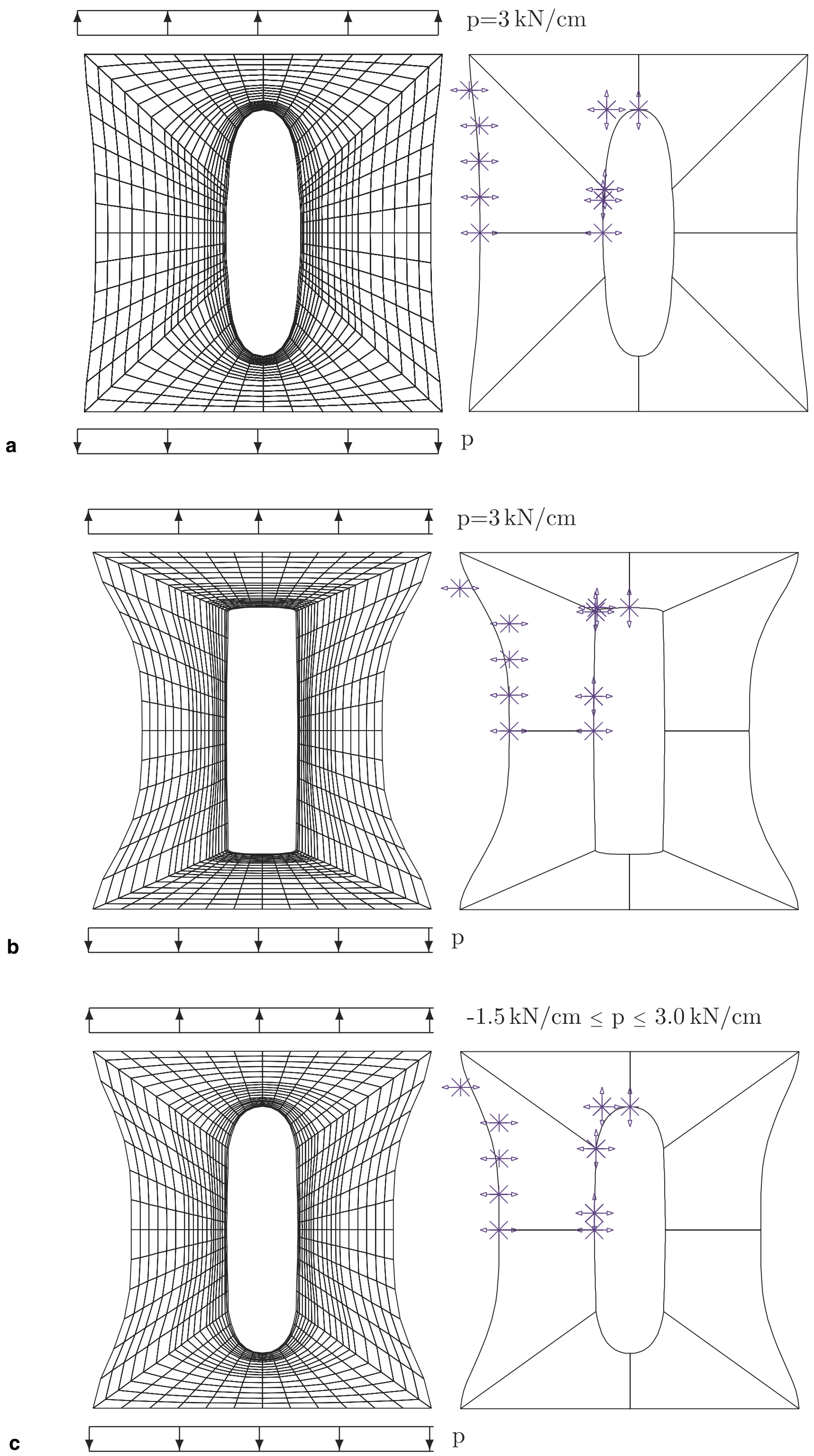

Fig. 9. Results for geometry and position of design variables for weight minimization of a plane stress problem under different conditions. (a) Elastic problem with one load case, (b) elasto-plastic problem with one load case and (c) shakedown problem with load domain.

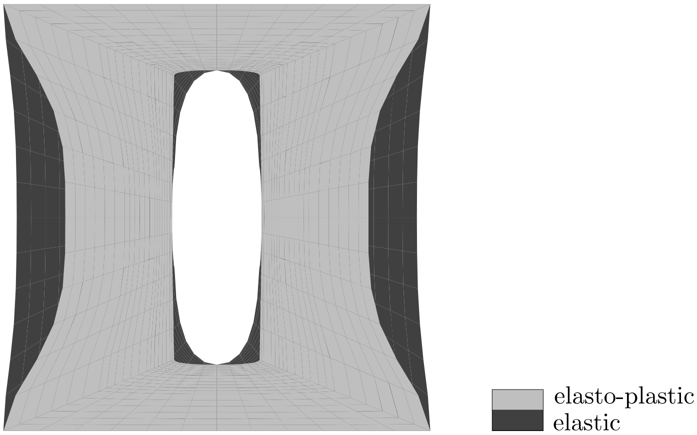

Fig. 10. Optimized geometries for elastic vs. elasto-plastic optimization.

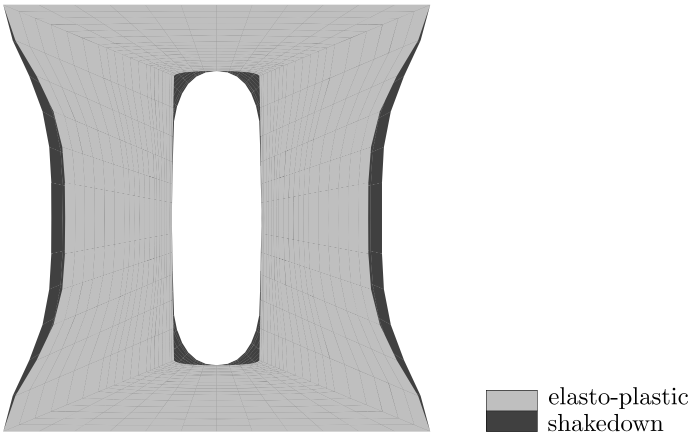

Fig. 11. Optimized geometries for elasto-plastic vs. shakedown optimization.

In Fig. 12 results of elastic and shakedown optimization are compared. The effect of an unlimited number of load cycles of elasto-plastic material in comparison with elastic material behavior for only one load case leads to the following conclusions. It can be seen that savings for shakedown optimization are considerably larger than for elastic optimization, while for both results the boundary of the hole remains smooth. The first result is due to the fact that hardening occurs for the shakedown problem and thus the material can be utilized more efficiently than for the elastic problem. The latter shows that the structural safety of the shakedown case is very close to that for the elastic case, whereas it is considerably higher than that for the elasto-plastic case.

6.2. Square plate with a central circular hole – optimizations with different load domains (proportional and non-proportional loading)

We consider once more a square plate with a central circular hole under plane stress condition. Material parameters and dimensions are those from Section 6.1, cf. Table 2 and Fig. 6. In this example the plate is loaded by two uniformly distributed and independently varying loads p_x and p_y in x- and y-direction, see Fig. 13a.

For this structure the following optimization problem is considered, cf. Table 5. The objective of the optimization is the reduction of weight G. A minimal shakedown factor of $\beta \geqslant 0.3$ is a constraint to the problem.

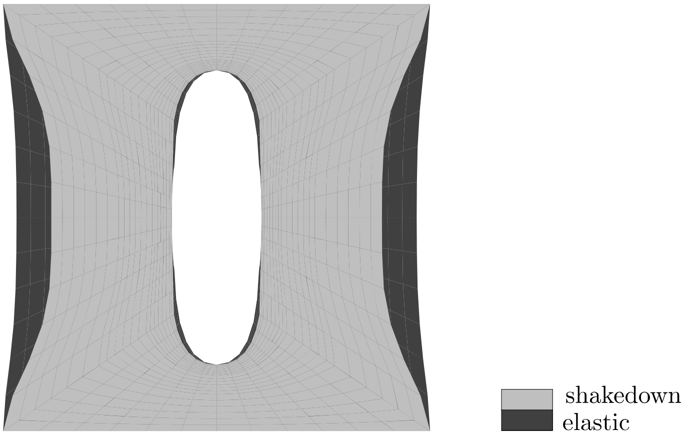

Fig. 12. Optimized geometries for elastic vs. shakedown optimization.

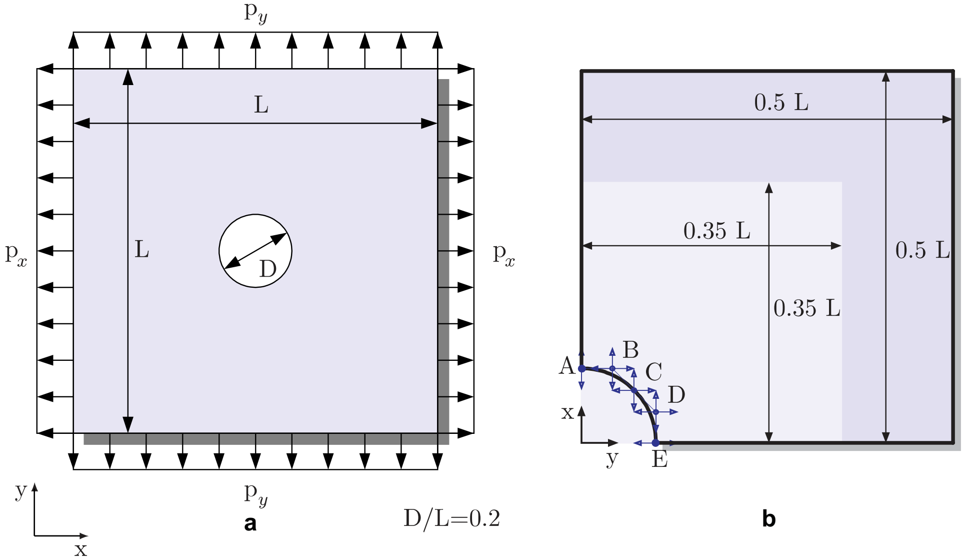

Fig. 13. (a) Geometry and loading conditions. (b) Design space.

For this example only the inner boundary of the central hole of the plate is varied. The design variables are eight coordinates of the control points of the Bézier curve defining the interior boundary. The chosen lower and upper bounds of the design variables are shown in Table 5. The corresponding design space is shown in Fig. 13b. The optimization is performed with three different load domains with proportional and non-proportional loading.

Table 5
Formulation of the optimization problem

Objective	Weight	$G \rightarrow \min$
Constraint	Shakedown factor	$\beta \geqslant 0.3$
Design variables	Control points	$DV = [y_A, x_B, y_B, x_C, y_C, x_D, y_D, x_E]$
	Bounds	$0.0L \leqslant \mathrm{DV}_i \leqslant 0.35L$
Loading	Bounds	$-0.5 \leqslant p_x \leqslant 1.0;\ -0.5 \leqslant p_y \leqslant 1.0$

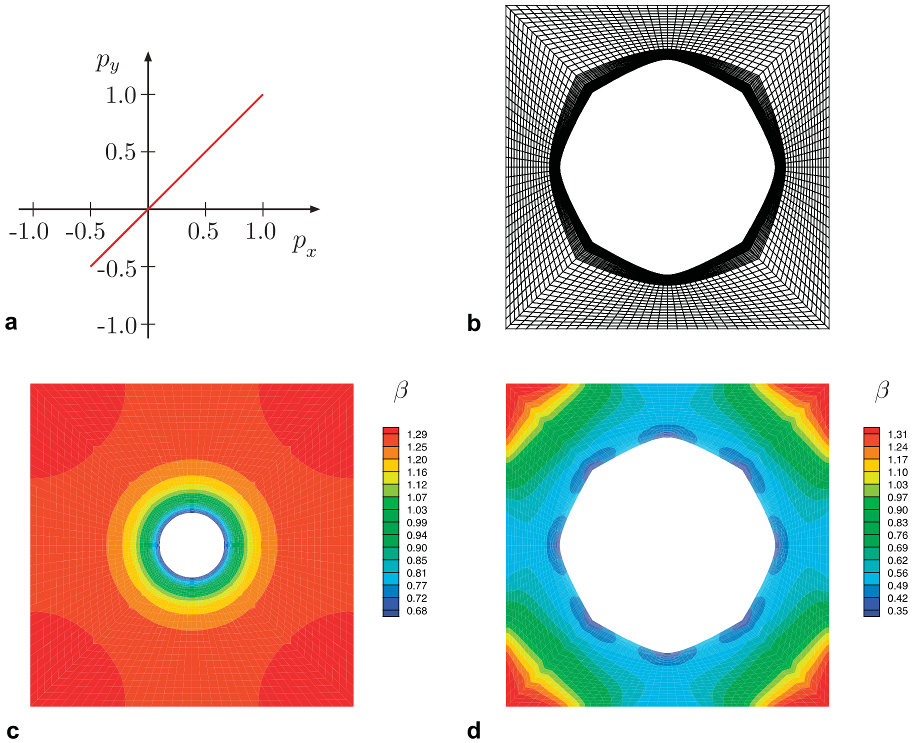

Fig. 14. Distribution of the shakedown factors for initial and improved geometry (proportional loading). (a) Load domain, (b) mesh of improved geometry, (c) initial geometry and (d) improved geometry.

Firstly, a load domain with two load vertices is considered, cf. Fig. 14a. The proportional loading of horizontal and vertical loads p_x and p_y varies between $-0.5 \leqslant p \leqslant 1.0$. For this example the distribution of the shakedown factor β for the initial design is shown in Fig. 14c. As can be seen the relevant shakedown factor $\beta \approx 0.6$ for this initial geometry can be found at the interior boundary of the hole. The optimized geometry and its corresponding distribution of shakedown factor can be seen in Fig. 14d. The symmetry of the structure is preserved which is due to the fact that equal bounds are considered for the two loads p_x and p_y. The resulting hole is not a circle anymore and it is not smooth. To the authors opinion this is due to the fact that the ratio of the diameter of the hole and the total dimension of the plate becomes larger during optimization such that the result of the optimization is influenced by the edges of the square plate.

A different result is obtained when non-proportional loading is considered. One example for non-proportional loading is the load domain with four load vertices as shown in Fig. 15a. For the initial design the distribution of shakedown factor β is shown in Fig. 15c. The minimal shakedown factor for the initial design is $\beta \approx 0.3$. Thus, only small savings can be achieved during optimization. Nevertheless, the size of the hole is increased slightly while its boundary remains smooth and the distribution of the shakedown factor β becomes more uniformly when compared with the initial distribution. Results for a non-symmetric load domain are shown in Fig. 16a–d. Again, a load domain with four load vertices is considered, cf. Fig. 16a, but its shape is not symmetric with respect to the bisector of the load domain. Thus, the resulting geometry of the plate is non-symmetric as well. But the boundary of the hole remains a smooth curve and savings are considerable. This is due to the fact that the shakedown factor $\beta \approx 0.55$ for the initial design which is considerably higher than the restraint of the optimization problem $\beta \geqslant 0.3$.

The results of the shape optimization of a square plate with a hole with non-proportional loading shows that for load domains with equal lower and upper bounds but different shape the resulting shapes of the varied inner boundary of the plate are very different. Thus for shape optimization of elasto-plastic structures it is of

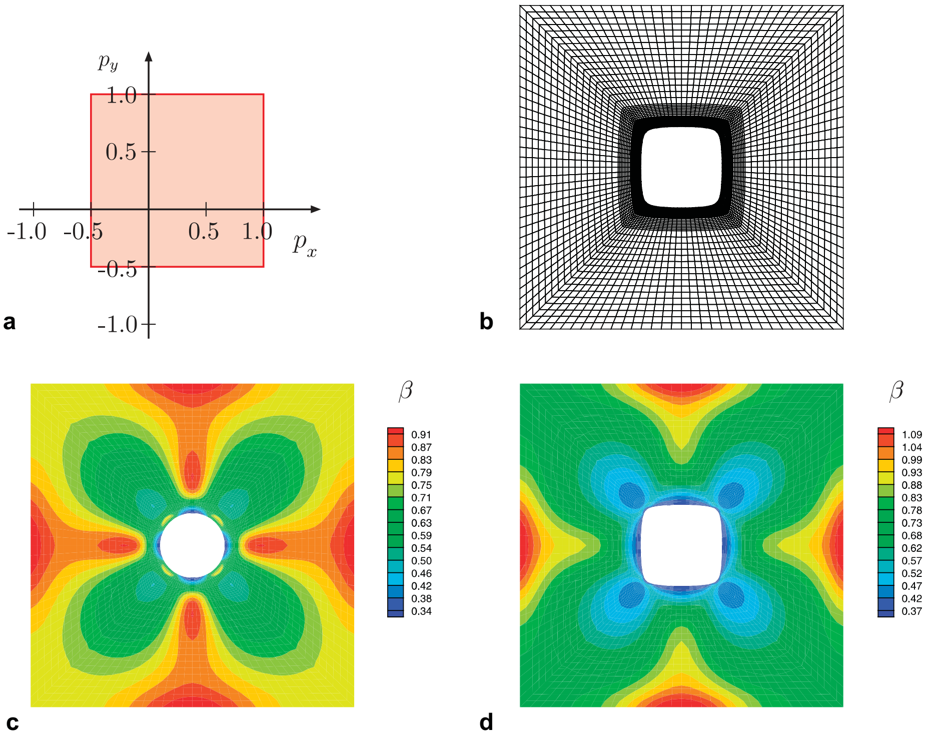

Fig. 15. Distribution of the shakedown factors for initial and improved geometry (non-proportional loading). (a) Load domain, (b) mesh of improved geometry, (c) initial geometry and (d) improved geometry.

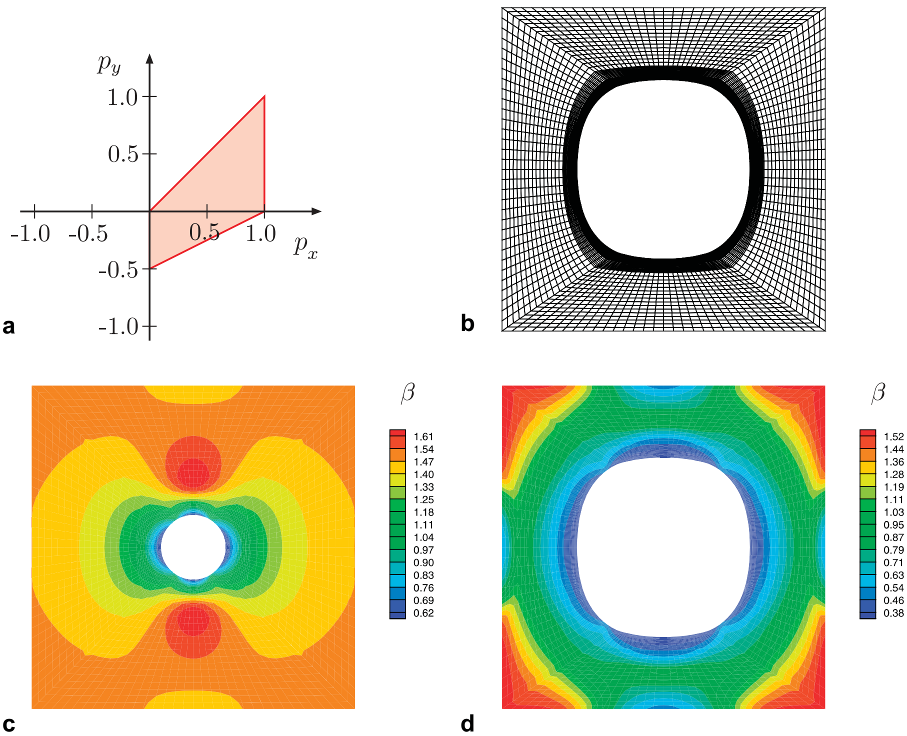

Fig. 16. Distribution of the shakedown factors for initial and improved geometry (non-proportional loading). (a) Load domain, (b) mesh of improved geometry, (c) initial geometry and (d) improved geometry.

great importance to consider not only single load cases but the correct load domain in order to derive reliable results.

Comparison of the results of the shape optimization for the non-proportional loading shows that the findings of the first example in Section 6.1 are confirmed. Generally, the resulting form of the hole remains a smooth curve. The level of structural safety is high due to the fact that arbitrary load paths within the considered load domains are admissible.

7. Conclusions

The proposed representation of variational design sensitivity describes an integrated treatment of all necessary linearizations in structural analysis and sensitivity analysis of shakedown problems. It is directed towards an easily applicable variational design sensitivity analysis and efficient numerical algorithms. The proposed methodology and the investigated problems are in line with our research on variational design sensitivity analysis described in Wiechmann et al. (1997), Barthold and Wiechmann (1997), Wiechmann and Barthold (1998) and Wiechmann et al. (2000).

The resulting geometries derived by optimization with shakedown constraints are adapted to arbitrary load paths and an unlimited number of load cycles in the whole load domain and not only to one single load case with a fixed load path. Comparison with results for problems with elastic and elasto-plastic deformations where only one load case is considered show that the level of structural safety as well as the savings derived in optimization with shakedown constraints are in-between these two limiting cases. If only elastic deformations are permitted during optimization the level of structural safety is high but savings are small due to the fact that utilization of the material is not optimal. On the other hand if elasto-plastic deformations are permitted the material is utilized optimally but only for the one load case that is considered. Thus savings are large but the level of structural safety is low. This indicates that the consideration of shakedown conditions when optimizing structures with elasto-plastic material behavior with multiple load cases is important for deriving robust and reliable designs.

References

Arora, J.S., 1993. An exposition of the material derivative approach for structural shape sensitivity analysis. Comput. Methods Appl. Mech. Eng. 105, 41–62.

Barthold, F.J., Stein, E., 1996. A continuum mechanical based formulation of the variational sensitivity analysis in structural optimization. Part I. Anal. Struct. Optim. 11, 29–42.

Barthold, F.J., Stein, E., 1997. Implementing variational design sensitivity analysis. In: Second World Congress of Structural and Multidisciplinary Optimization. pp. 181–186.

Barthold, F.J., Wiechmann K., 1997. Variational design sensitivity for inelastic deformation. In: Proceedings of the COMPLAS 5, Barcelona, pp. 792–797.

Belytschko, T., 1972. Plane stress shakedown analysis by finite elements. Int. J. Mech. Sci. 14, 619–625.

Bleich, H., 1932. Über die Bemessung statisch unbestimmter Stabwerke unter der Berücksichtigung des elastisch-plastischen Verhaltens der Baustoffe. Bauingenieur 13, 261–267.

Céa, J., 1981. Problems of shape optimal design. In: Optimization of Distributed Parameter Structures. Sijthoff & Noordhoff, pp. 1005–1048.

Corradi, L., Maier, G., 1973. Inadaptation theorems in the dynamics of elastic-workhardening structures. Ing. Arch. 43, 44–57.

Corradi, L., Zavelani, I., 1974. A linear programming approach to shakedown analysis of structures. Comput. Math. Appl. Mech. Eng. 3, 37–53.

Gokhfeld, D.A., Cherniavsky, O.F., 1980. Limit Analysis of Structures at Thermal Cycling. Sijthoff & Noordhoff.

Kaliszky, S., Lógó, J., 1997. Optimal plastic limit and shakedown design of bar structures with constraints on plastic deformation. Eng. Struct. 19 (1), 19–27.

Kaliszky, S., Lógó, J., 2002. Layout and shape optimization of elastoplastic disks with bounds on deformation and displacement. J. Mech. Struct. Mach. 3 (2), 177–191.

Koiter, W.T., 1956. A new general theorem on shakedown of elastic–plastic structures. Proc. Koninkl. Acad. Wet. 59, 24–34.

König, J.A., 1966. Theory of shakedown of elastic–plastic structures. Arch. Mech. Stos. 18, 227–238.

König, J.A., 1969. A shakedown theorem for temperature dependent elastic moduli. Bull. Acad. Polon. Sci. Ser. Sci. Tech. 17, 161–165.

Leckie, F.A., 1965. Shakedown pressure for flush cylinder-sphere shell interaction. J. Mech. Eng. Sci. 7, 367–371.

Maier, G., 1972. A shakedown matrix theory allowing for workhardening and second-order geometric effects. In: Proceedings of the Symposium Foundations of Plasticity, Warsaw.

Melan, E., 1938a. Der Spannungszustand eines Mises-Henckyschen Kontinuums bei veränderlicher Belastung. Sitzber. Akad. Wiss. Wien IIa 147, 73–78.

Melan, E., 1938b. Zur Plastizität des räumlichen Kontinuums. Ing. Arch. 8, 116–126.

Nguyen Dang, H., Morelle, P., 1981. Numerical shakedown analysis of plates and shells of revolution. In: Proceedings of 3rd World Congress and Exhibition on FEMs. Beverly Hills.

Polizzotto, C., Borino, G., Caddemi, S., Fuschi, P., 1991. Shakedown problems for material models with internal variables. Eur. J. Mech. A/Solids 10, 787–801.

Prager, W., 1956. Shakedown in elastic–plastic media subjected to cycles of load and temperature. In: Proc. Symp. Plasticita nella Scienza delle Costruzioni, Bologna.

Sawczuk, A., 1969a. Evaluation of upper bounds to shakedown loads of shells. J. Mech. Phys. Solids 17, 291–301.

Sawczuk, A., 1969b. On incremental collapse of shells under cyclic loading. In: Second IUTAM Symposium on Theory of Thin Shells. Kopenhagen. Springer Verlag, Berlin.

Shen, W.P., 1986. Traglast- und Anpassungsanalyse von Konstruktionen aus elastisch, ideal plastischem Material. PhD thesis, Inst. für Computeranwendungen, Universität Stuttgart.

Stein, E., Zhang, G., 1992. Theoretical and numerical shakedown analysis for kinematic hardening materials. In: 3rd Conference on Computational Methods in Mechanics and Engineering, Barcelona.

Stein, E., Zhang, G., Mahnken, R., König, J.A., 1990. Micromechanical modeling and computation of shakedown with nonlinear kinematic hardening including examples for 2-D problems. In: Proceedings of the CSME Mechanical Engineering Forum, Toronto, pp. 425–430.

Stein, E., Zhang, G., König, J.A., 1992. Shakedown with nonlinear hardening including structural computation using finite element method. Int. J. Plast. 8, 1–31.

Stein, E., Zhang, G., Mahnken, R., 1993. Shake-down analysis for perfectly plastic and kinematic hardening materials. In: Progress in Computational Analysis of Inelastic Structures. Springer Verlag, pp. 175–244.

Tortorelli, D.A., Wang, Z., 1993. A systematic approach to shape sensitivity analysis. Solids Struct. 3 (9), 1181–1212.

Weichert, D., 1986. On the influence of geometrical nonlinearities on the shakedown of elastic–plastic structures. Int. J. Plast. 2, 135–148.

Wiechmann, K., Barthold, F.J., 1998. Remarks on variational design sensitivity analysis of structures with large elasto-plastic deformations. In: Proceedings of the 7th AIAA/USAF/NASA/ISMO Symposium on Multidisciplinary Analysis and Optimization, St. Louis, pp. 349–358.

Wiechmann, K., Barthold, F.J., Stein, E., 1997. Optimization of elasto-plastic structures using the finite element method. In: Second World Congress of Structural and Multidisciplinary Optimization, pp. 1013–1018.

Wiechmann, K., Barthold, F.J., Stein, E., 2000. Shape optimization of shakedown analysis problems. In: Inelastic Analysis of Structures under Variable Loads: Theory and Engineering Applications. Kluwer, pp. 49–68.

Zolésio, J.P., 1981. The material derivative (or speed) method for shape optimization. In: Optimization of Distributed Parameter Structures. Sijthoff & Noordhoff, pp. 1088–1151.